

# Experimental and numerical validation of an analytical hydro-plastic model for the prediction of structural damage in extreme water slamming

Zhaolong Yu, Anni Cao & Jørgen Amdahl

*Centre for Autonomous Marine Operations and Systems (AMOS), Norwegian University of Science and Technology (NTNU), Norway*

*Department of Marine Technology, Norwegian University of Science and Technology (NTNU), Norway.*

**ABSTRACT:** Extreme water slamming poses great threats on the safety of ships and offshore structures at sea, which may in the extreme conditions cause large structural damage, progressive collapse of structures and even fatalities. The interaction between hydrodynamic loads and large plastic structural deformation termed as hydro-plastic slamming, however, has not been well understood. Recently, Yu et al. (2019a) proposed an analytical hydro-plastic model for the prediction of permanent deflections of beams and stiffened panels in extreme water impacts and verified the model by numerical simulations. This paper aims for further verification of the hydro-plastic model by comparison with recent drop tests of aluminum plates carried out by Sintef Ocean and numerical simulations of water impacts on a semi-submersible column using the Arbitrary Lagrangian Eulerian (ALE) method. The drop tests focus on water impacts of bare plates while the ALE simulations yield plastic damage of stiffened panels. Experimental set-up of the drop tests and numerical modelling of water impacts on the semi-submersible column are described. Structural damage of plates and stiffened panels from the experiments and numerical simulations respectively are used to verify the hydro-plastic model. Its validity and accuracy are discussed.

**Keyword:** hydro-plastic slamming; analytical solution; beams and stiffened panels; permanent deflection; validation

## 1 INTRODUCTION

Ships and offshore structures will unavoidably experience water impacts during its service lifetime. Water impacts are characterized by high local pressures and short durations. The highly impulsive loads will threaten significantly the safety of structures. In 2015, the offshore drilling rig *COSL Innovator* was hit by a steep energetic horizontal wave. The accident led to extensive damage to the cabins and death of one cabin crew. This raises great concern on the design against such extreme wave impacts. Shortly after the incident, two design guidelines DNVGL-OTG-13 (2016) and DNVGL-OTG-14 (2016) have been developed as a first approach to address and reflect the severity of wave in deck events.

Structures subjected to impulsive loads from water slamming, may respond in the elastic or elasto-plastic regimes depending on the load intensity. There can be significant coupling effect between water pressure and the structural response, termed as hydroelasticity and hydro-elastoplasticity, respectively. Hydroelastic slamming has been studied extensively, for instance by Faltinsen (2000), Kvalsvold and Faltinsen (1995), Bishop and Price

(1979) and Qin and Batra (2009), but similar attention has not been given to the hydro-elastoplastic or hydro-plastic slamming. In practice, offshore structures may be impacted by steep and energetic waves in extreme sea states, causing significant structural damage.

The mechanics and physics of hydro-elastoplastic slamming has not been fully understood from the literature. Traditional methods often assume temporal and spatial distribution of design slamming loads, and apply the loads on the structures to get structural responses, e.g. in the guidelines DNVGL-OTG-13 (2016) and DNVGL-OTG-14 (2016). Similarly, a few researchers studied plastic response of structures subjected to extreme slamming by assuming a certain temporal and spatial pressure distribution, such as Jones (2011), Jiang and Olson (1995) and Henke (1994). The methods, however, neglect the hydro-elastoplastic coupling effect between structural responses and water pressure, and do not reveal the governing physics.

Recent studies have shown new developments on the coupled hydro-plastic slamming phenomenon. Yu et al. (2019a) proposed an analytical solution for

the hydro-plastic response of beams and stiffened panels subjected to extreme water slamming. The model was verified of good accuracy by comparison with ALE simulations (Yu et al., 2019b). Travelling hinges were found crucial for structural responses under impulsive loads, and this made the deformation pattern quite different from an elastic structure. More coupled ALE simulations of stiffened panels with plastic damage can be found in Truong et al. (2020) and Cheon et al. (2016). Experiments and model tests are among the most valuable tools for understanding the physical effects of the slamming phenomena. Experimental data is also crucial for validation of numerical tools and theoretical methods.

Abrahamsen et al. (2020) carried out drop tests of aluminum plates at the ocean basin of Sintef Ocean. The plates are very thin walled so to produce large plastic deformations during water impacts. The Digital Image Correlation (DIC) technique with high-speed cameras is adopted to track deformation of the plates during the impact. The video from the experiment shows considerable interaction effects between structural response and hydrodynamics and cavitation effects. Abrahamsen et al. (2020) also presented a hydro-plastic model for the prediction of permanent deflections of plates during water impacts and validated the model with experiments.

This paper aims for further verification and validation of the hydro-plastic model proposed by Yu et al. (2019a) using the experimental data by Abrahamsen et al. (2020) for slamming of plates and more ALE simulations of stiffened structures. The predicted structural damage using the hydro-plastic model will be compared with experimental and numerical results and discussed.

## 2 ANALYTICAL MODEL FOR HYDRO-PLASTIC SLAMMING

### 2.1 The analytical model for hydro-plastic slamming

The 2D hydro-plastic model by Yu et al. (2019a) assume that in the extreme water impacts, the elastic energy of a structure is small compared to the plastic energy such that all the kinetic energy should be dissipated by plastic deformations. During extreme water slamming of beams at a small impact angle, the response is categorized into two phases, i.e. the structural inertia phase (also called the acoustic phase) and the free deflection phase. In the structural inertia phase, the structure is subjected to an intensive pressure impulse with a large pressure peak and a short duration. At the end of the structural inertia phase, the structure is assumed to be imparted a deformation velocity equal to the initial drop velocity  $V_0$  in the beam middle portion between the two

travelling hinges. The deformation velocity decreases linearly to zero from the travelling hinges to the beam ends. The duration of the structural-inertia phase is, however, too short for the structure to build up any deflection. These are considered as initial conditions of the free deflection phase.

In the free deflection phase, the structure deforms and may experience three possible deformation stages, i.e. the travelling hinge stage 1, the stationary hinge stage 2 and the pure tension stage 3 (refer Fig. 1). In stage 1, travelling hinges form at a certain distance  $X$  from the beam ends and move towards the middle. The beam portion between the hinges has a constant velocity  $V_m$  equal to the initial impact velocity  $V_0$  (refer Fig. 1(a)). When the travelling hinges merge in the middle, the stationary hinge stage 2 starts and the beam middle velocity starts to decrease over time. During the deflection, the beam bending moment and axial membrane force interact through the generalized interaction curves. For stiffened panels, the interaction functions are taken from Yu et al. (2018). For beams fixed at the ends, when the beam middle deflection  $\delta$  reaches the beam height  $h$ , the beam cross section becomes fully occupied by membrane forces, and the pure tensile stage 3 starts. Permanent deflection is reached when the beam middle velocity  $V_m$  decreases to zero.

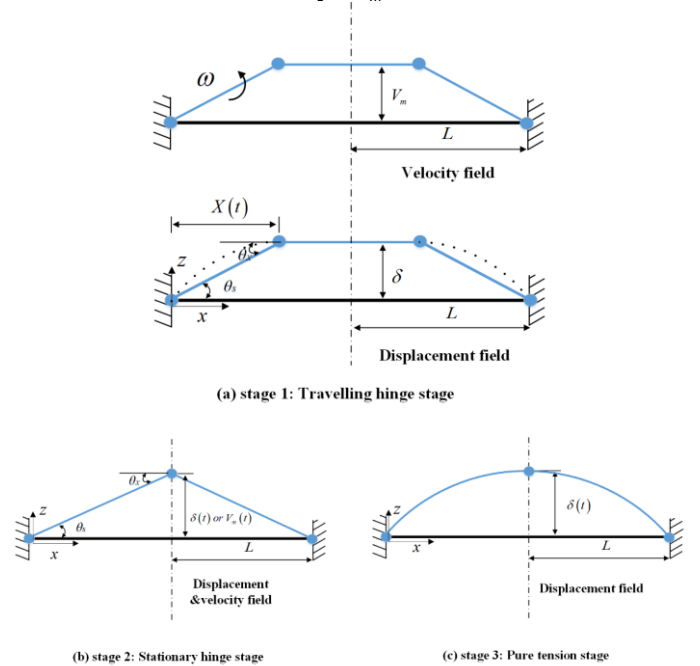


Fig. 1. Deformation stages of a beam during the free-deflection phase induced by slamming

During the deformations, significant coupling exists between the beam plastic deflection and the water pressure, denoted as hydro-plasticity. In stages 2 and 3, water pressure acts as an added mass effect and pushes the decelerating structure to deform. For stage 1, apart from an added-mass term, we have a second pressure term related to an added-mass time change effect due to the moving hinges leading to a change in the structural mode. By equating the rate

of internal and external works, the governing motion equations are found, and are solved numerically.

## 2.2 Governing non-dimensional parameters

For the hydro-plastic slamming response of flat plate strips, i.e. of two-dimensional (2D) flat plates, three governing non-dimensional parameters have been identified, which are,

- The non-dimensional velocity

$$V_{nd} = V_0 \sqrt{\frac{\rho L^3}{M_0 h / b}}$$

- The mass ratio  $m_{nd} = m / \rho b L$
- The ratio of initial travelling hinge position over half of the beam length

$$X_{nd} = \frac{X(t=0)}{L} = \sqrt{\frac{24}{\left(V_0 \sqrt{\frac{\rho L^3}{M_0 h / b}}\right)^2} \cdot \frac{V_0 L}{c_e h}}$$

For the hydro-plastic response of stiffened panels, two more parameters are identified in addition to the three above:

- The area ratios:

$$A_{ps,nd} = A_p / A_s \quad \text{and} \quad A_{wt,nd} = A_w / A_t$$

Here,  $V_0$  is the initial impact velocity,  $\rho$  is the water density and  $L, b, h$  are, respectively, the length, width and height of the beam.  $m$  is the mass of a beam per unit length,  $X(t=0)$  is the initial position of a travelling hinge from the corresponding beam edge.  $M_0$  is the fully plastic bending moment for the beam cross section.  $M_0 = 1/4 \sigma_y b h^2$  for rectangular beams and  $M_0 = \sigma_y (A_t + A_w / 2) h$  for stiffened panel cross sections.  $A_p, A_w, A_t$  are the area of the plate flange, area of the web and area of the top flange, respectively.  $A_s = A_t + A_w$  is the area of the stiffener.

It is found that the non-dimensional velocity  $V_{nd}$  is the most crucial parameter that dominates the hydro-plastic response of beams and stiffened panels. Stiffened panels with large web heights,  $h$ , are mainly governed by stages 1 and 2 deformations. The permanent deflection increases nonlinearly with the non-dimensional velocity. For plates, the characteristic dimension i.e. the plate thickness  $h$  is much smaller than the stiffener spacing, and the response is mainly governed by stage 3.  $\delta_p / h$  increases virtually linearly with the non-dimensional velocity.

The area ratios  $A_p / A_s$  and  $A_w / A_t$  are important parameters for stiffened panels. Permanent deflections increase with decreasing  $A_p / A_s$  and  $A_w / A_t$  ratios for a given non-dimensional velocity, and the  $A_p / A_s$  ratio is dominant. The influences of the mass ratio  $m / \rho b L$  and the  $X(t=0) / L$  ratio are generally limited.

## 3 EXPERIMENTAL VALIDATION WITH DROP TESTS OF PLATES WITH PLASTIC DAMAGE

### 3.1 Drop tests of plates with plastic damage by Abrahamsen et al. (2020)

Drop tests of unstiffened plates by Abrahamsen et al. (2020) will be used to validate the proposed hydro-plastic model. The experiments were carried out in the Ocean Basin Laboratory at Sintef Ocean. The aluminum plates had an effective plate area of 22 x 22 cm<sup>2</sup> and were embedded in a strong steel box that can be considered as rigid, refer to Fig. 2(a). The plate thickness was 0.6 mm. The steel box was bolted to the bottom of the rigid impactor. The impactor was open on top and had a quadratic opening in the bottom, which allows visual monitoring of the structural response of the aluminum plate. The steel box was connected to a rigid arm by a hinge. The impact angle between the plate and water surface at the instant of water entry could be adjusted at the hinge. The experimental set-up is shown in Fig. 2(b). The total weight of the drop test rig was 139.42 kg, which was considered sufficiently heavy to ensure the rigid body deceleration was small at the instant of water entry.



Fig. 2. (a) Test specimen of aluminum plates; (b) setup of the drop test, from Abrahamsen et al. (2020).

The 0.6-mm-thick aluminum plate was manufactured from low-strength, strain-hardened, and cold-rolled sheets of the commercial alloy EN AW 1050A-H111. Tensile tests were carried out with several test specimens cut directly from plates after test along the length and width direction. The obtained stress strain curves are shown in Fig. 3 from Abrahamsen et al. (2020). The material exhibited

significant hardening with a yield stress of about 20 MPa and an ultimate stress of 65 MPa.

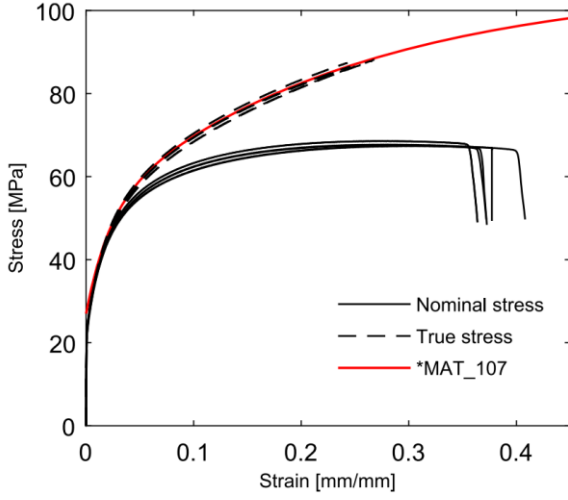


Fig. 3. True stress and engineering stress of the aluminum obtained from tensile tests extracted from Abrahamsen et al. (2020).

Abrahamsen et al. (2020) carried out drop tests with two impact angles of  $0^\circ$  and  $4^\circ$  and different drop heights. The cases were defined in Table 1. The Digital Image Correlation (DIC) technique with high-speed cameras was applied to measure deformation of the plates during the impact. The DIC measurement was compared with permanent deflections of the plates measured by a dial gauge after tests in Abrahamsen et al. (2020) and showed good accuracy.

Table 1. Cases for drop tests by Abrahamsen et al. (2020)

Test no.	Impact angle	Drop height	Measured rigid body velocity at the instant of water entry (m/s)
1	0	443	3.11
2	0	443	3.11
3	0	443	3.11
4	0	118	1.61
5	0	222	2.21
6	0	778	4.11
7	0	778	4.11
8	0	778	4.11
9	4	444	3.11

### 3.2 Validation of the hydro-plastic model by the drop tests

Fig. 4 compares the central point deflection from the drop tests experiment and the predictions by the hydro-plastic model. Due to significant hardening effects of the aluminum material (refer to Fig. 3), three characteristic flow stresses are adopted as done in Abrahamsen et al. (2020), namely the initial yield stress 20 MPa, the ultimate stress 65 MPa and an av-

erage of the two 42.5 MPa. The average flow stress is considered more reliable as inputs for the theoretical model here due to the significant material hardening effect. Results show that the deflection predicted by the hydro-plastic model agrees quite well with the experimental curves. The model captures well the temporal evolution of plate deflections in both phases and magnitudes. The model using an average flow stress of 42.5 MPa yields the best match.

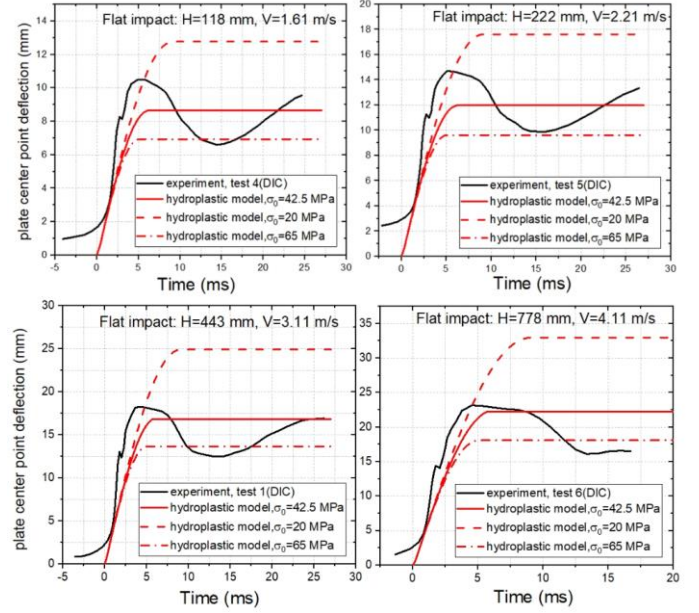


Fig. 4. Comparison of the central point deflection of plates from drop tests by Abrahamsen et al. (2020) and predictions with the hydro-plastic model by Yu et al. (2019a)

Fig. 5 compares the shape of deflection at the cross section of maximum deflection for the case *flat impact* -  $H=443$  mm,  $V=3.11$  m/s from the experiments and the hydro-plastic models by Abrahamsen et al. (2020) and Yu et al. (2019a). In the experiment, the plate was quite thin compared to the plate length, and the plate quickly goes into the pure tension stage. The plate then behaves more like a string with a sinusoidal deflection profile. The deflection shape predicted by the hydro-plastic model by Yu et al. (2019a) agrees well with the experimental curve. The model by Abrahamsen et al. (2020) assumes linear deflection and shows some differences.

The hydro-plastic model by Yu et al. (2019a) indicates that the permanent deflection of plates in extreme water slamming is governed by a non-dimensional velocity  $V_0 \sqrt{\rho L^3 / M_0 h}$ , where  $V_0$  is the velocity at the instant of water entry,  $\rho$  is the water density,  $2L$  is the plate length,  $M_0 = 1/4 \sigma_0 h^2$  is the plastic bending moment of a plate strip with unit width,  $h$  is the plate thickness. The nondimensional permanent deflection  $\delta_p / h$  varies virtually linearly with the non-dimensional velocity  $V_0 \sqrt{\rho L^3 / M_0 h}$  according to the theory as shown in Fig. 6. The linear trend is confirmed by the experimental data and

permanent deflections predicted by the model agree well with experiments.

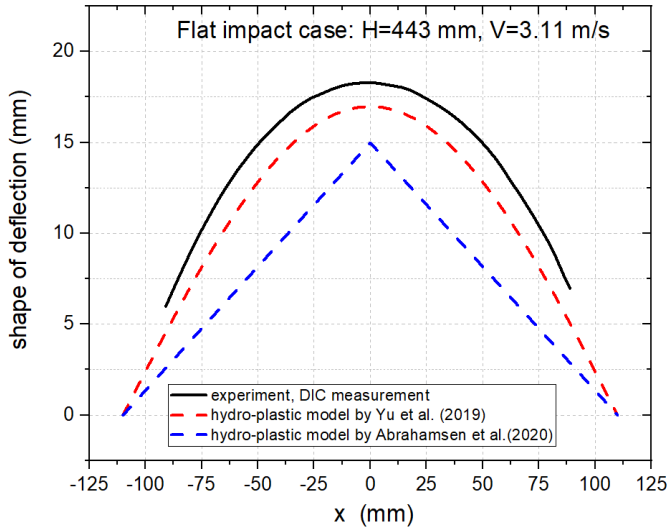


Fig. 5. Deflection profile of plates at the cross section of maximum deflection from experiments and hydro-plastic models

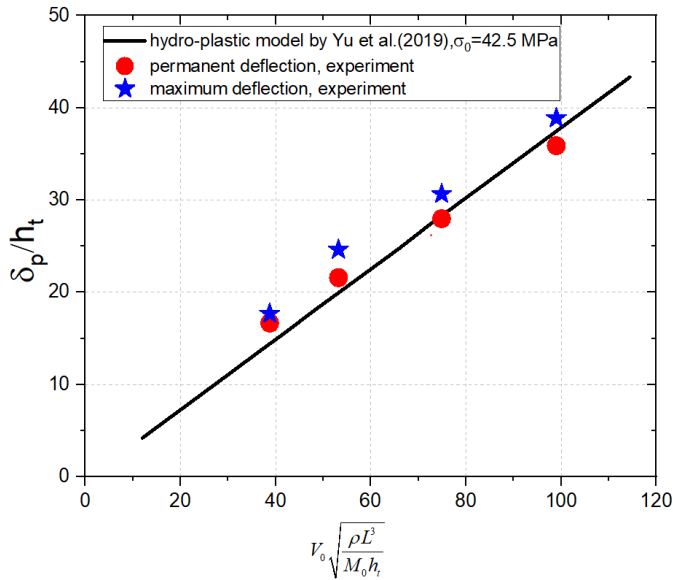


Fig. 6. Variation of non-dimensional permanent deflection with non-dimensional velocity by the hydro-plastic model and the experiments

Figs. 7 (a) and (b) plots the time history of plate deflection at the plate center and plate deflection profile at the plate center line, respectively. The drop height is 443 mm. The plots are extracted from experiments by Abrahamsen et al. (2020). Travelling hinges are not directly observed because the plate is very thin walled (0.6 mm), and the plate deformation quickly goes into the pure tension stage 3 as defined by Yu et al. (2019a). This gives a sinusoidal like deflection profile. More experiments with thicker plates will be needed to validate the travelling hinge concept. Fig. 7 (c) shows the picture taken from underwater high speed camera by Abrahamsen et al. (2020). Significant water cavitation and fluid structure interactions during water impacts are observed.

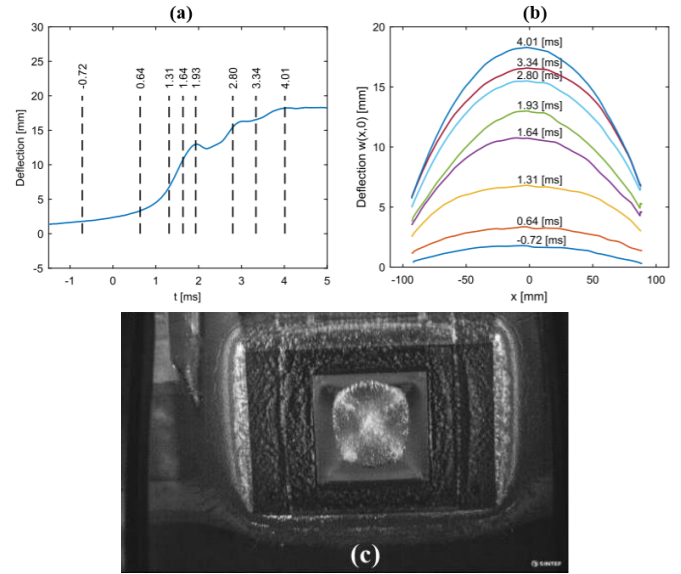


Fig. 7. (a) deflection of plate center in the 'rapid deflection stage', (b) profile of deflection at the center line. (c) pictures during water impact taken by the underwater high-speed camera. The drop height is 443 mm. The pictures are extracted from Abrahamsen et al. (2020).

## 4 NUMERICAL VERIFICATION OF THE HYDRO-PLASTIC MODEL USING ALE SIMULATIONS OF PLATFORM COLUMN SLAMMING

### 4.1 Description of the semi-submersible column model

The column of a typical semi-submersible platform in the North Sea is selected, refer to Fig. 8. The model spans over three decks in the vertical direction, including the top deck at around EL.51000mm level, the secondary deck at around EL.31500mm level and the third deck at EL.20000mm level. The model is therefore 31 m high and is considered sufficiently large to capture global responses in slamming analysis. The outer plate of the platform column has a thickness of 16 mm, and is equipped with HP stiffeners with dimensions of 260 mm×10 mm×37 mm×27.3 mm. The stiffener spacing is 625 mm. The Transverse girders are T-girders with dimensions 1000 mm ×16 mm×300 mm×20 mm. The spacing between transverse girders is 2100 mm. The deck plates have a plate thickness of 12 mm and are equipped with bulb stiffeners of HP 220mm×10mm.

### 4.2 Numerical set-up of ALE simulations

The water and air domains are a 9 m×9 m ×2.875 m area located at the second deck above the waterline, which covers more than 3 spans of girders. Water and air are modelled with multi-material Eulerian meshes while the structure is modelled with Lagrangian meshes. A uniform mesh size of 60 mm is used

for both the structures and fluids, which is considered to quite fine. Coupling is enabled in a way that the Lagrangian structure domain imposes displacement and velocity boundary conditions on the Eulerian fluid, which in return imposes hydrodynamic pressure on the structure. The water and air domains are modelled using the 1-point ALE multi-material solid elements. Material properties of the fluids are defined with the NULL materials and EOS (equation of state). The EOS state properties adopted for water and air are listed in Table 2.

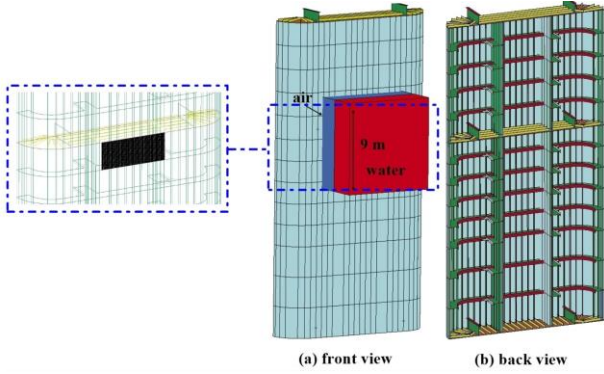


Fig. 8. The column structure of a semi-submersible platform

The penalty-based coupling method is applied to model contact between the fluid and the structure. During contact, the fluid nodes are allowed to have a small penetration into the structure. Resisting forces are then imposed between the contact points on the structural elements and the fluid nodes. The coupling is limited only to the local fluid-structure contact region as marked in black in Fig. 8 while no coupling is defined elsewhere. The penalty factor corresponding to the contact stiffness of interacting bodies is set to the default value of 0.1. The contact damping is selected to be 0.9 times the critical damping. The steel material with a yield stress of 355 MPa is used. The power law parameters for the material are shown in Table 3. The simulation is carried out in a way like a drop test, where the column structure is given a constant velocity at the rear side and impacts the water.

Table 2. EOS parameters for water and air

EOS-Linear polynomial	Air	EOS GRUNEISEN	Water
Density (kg/m <sup>3</sup> )	1.225	C	1025
C <sub>0</sub>	0	S1	1.647e+3
C <sub>1</sub>	0	S2	1.921
C <sub>2</sub>	0	S3	-0.096
C <sub>3</sub>	0	GAMA0	0.35
C <sub>4</sub>	0.4	A	0
C <sub>5</sub>	0.4	-	
C <sub>6</sub>	0	-	
E <sub>0</sub>	2.5e+5	E <sub>0</sub>	2.895e+5
V <sub>0</sub>	1	V <sub>0</sub>	1

Table 3. Material properties for the plates and stiffened panels

Material	Hardening type	$\sigma_y$ (MPa)	$K$ (MPa)	$n$
steel	Power law	355	780	0.16

### 4.3 ALE simulation results and verification of the hydro-plastic model

In extreme environmental conditions, instant water impact velocity can reach 20 m/s. Drop tests with an impact velocity are carried out with two impact angles of 0 deg and 3 deg, respectively. The resulting water pressure and stiffened panel deflection at the panel center are plotted in Fig. 9. The water jets of the two cases are shown in Fig. 10. Fig. 11 plots the corresponding local structural damage on the platform column.

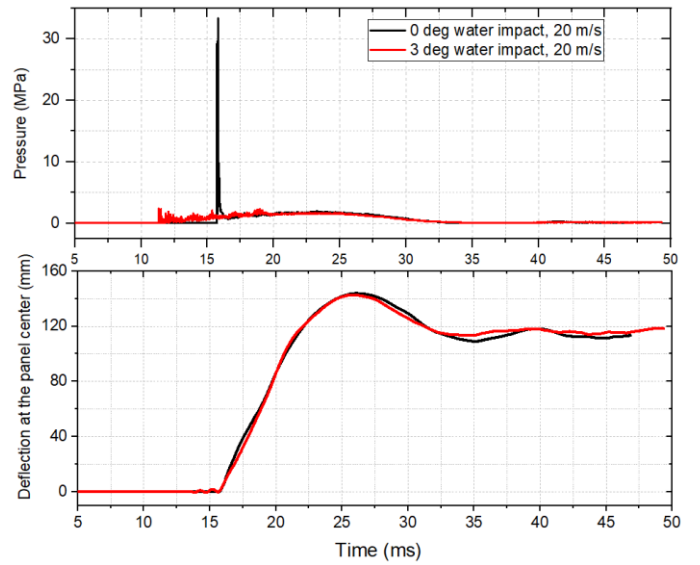


Fig. 9. Water pressure and stiffened panel deflections during water impact with an impact velocity of 20 m/s and two different impact angles of 0 deg and 3 deg.

The water pressures show significant differences at the initial stage of water entry. The 0 deg water impact case yields a very large pressure peak of 33.3 MPa (which is needed to retard the plate to zero speed) while the peak pressure for the slightly inclined impact case is significantly smaller. The water pressures during panel deflections are, however, quite similar. The two cases also yield very similar panel deflections. This confirms the fact that the magnitude of the initial peak pressure is not important for structural responses. The part that matters is the total impulse in the initial excitation phase, which is the area below the pressure curve. The 3 deg water impact case yields slightly asymmetric water spay compared to the flat impact. Both cases cause significant permanent damage on the structures, refer to Fig. 11.

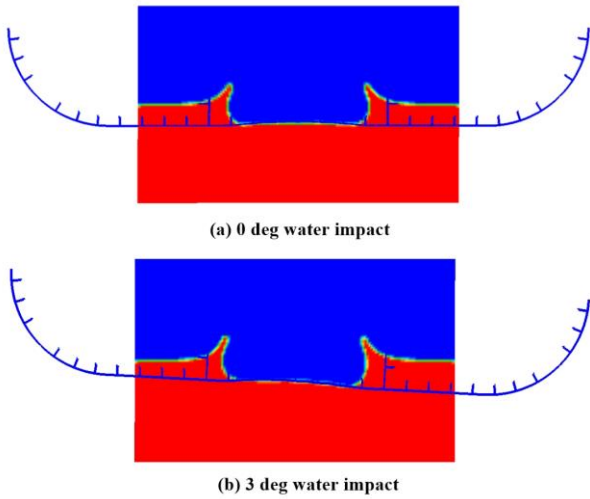


Fig. 10. Water jets during slamming with two different impact angles

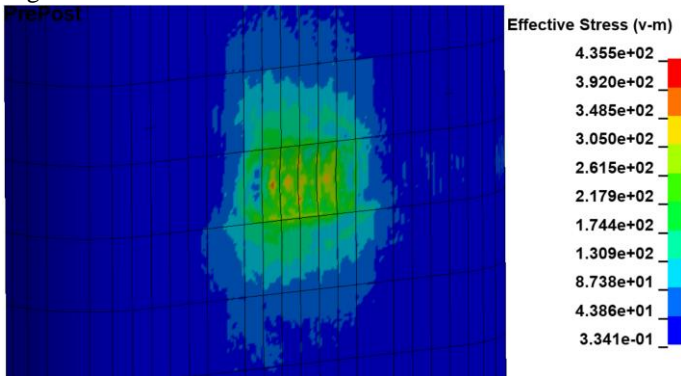


Fig. 11. Local damage on the stiffened panel of the platform column after water impacts with an impact velocity of 20 m/s

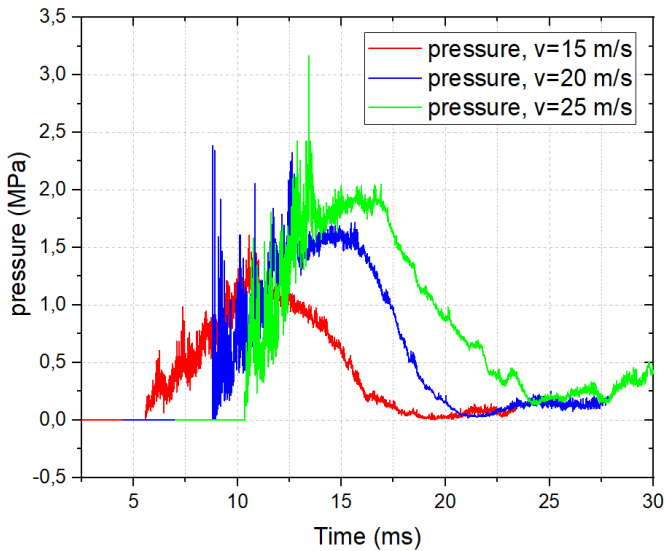


Fig. 12. Water pressure during slamming on the stiffened panel of the platform column with different impact velocities and an impact angle of 3 deg

Water impacts with three different velocities of 15 m/s, 20 m/s and 25 m/s are carried out with an impact angle of 3 deg. The corresponding average water pressure is plotted in Fig. 12. The pressure increases with drop velocities and the initial peaks are not obvious. Fig. 13 compares stiffened panel deflections by ALE simulations and the hydro-plastic model for the three different velocities. Quite good agreement is obtained for the permanent deflections

in all the three cases. Stiffened panels are characterized by the web plating with large heights, and their deformation patterns are governed by the stationary hinge in stage 2. The good correlation with numerical results demonstrates good accuracy of the hydro-plastic model for stiffened panels of realistic platform forms.

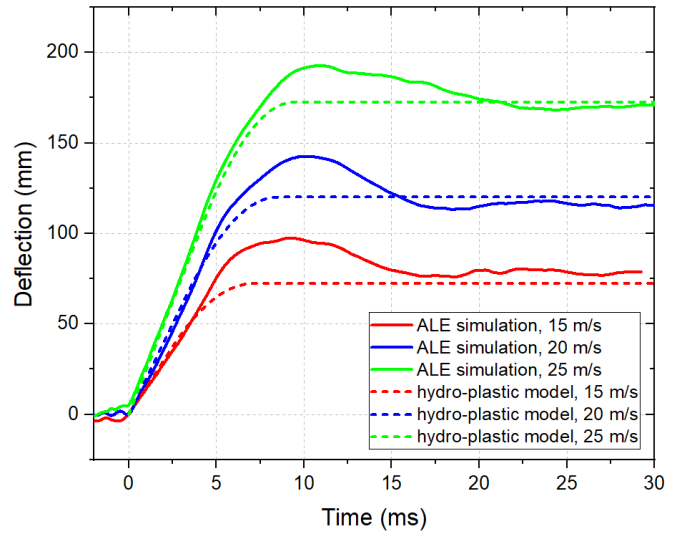


Fig. 13. Comparison of panel deflections by ALE simulations and the hydro-plastic model during water impacts with different impact velocities and an impact angle of 3 deg

## 5 CONCLUSIONS

This paper presents further validation and verification of a hydro-plastic model by comparing with the results of drop tests of thin aluminum plates carried out by Sintef Ocean and numerical simulations of water impacts on a semi-submersible column.

The comparison with the drop tests showed that the hydro-plastic model captures the development of the plate deflections in both magnitude and phase. The deformation profile correlates also well with experiments. The deformations of the thin plates under water impacts are generally governed by the pure tension stage 3. Hence, The Sintef Ocean drop tests demonstrate the validity and good accuracy of stage 3 of the hydro-plastic model.

The comparison with numerical simulations of water impacts on a semi-submersible platform column, shows that the hydro-plastic model predicts well the development of stiffened panel deflections. Stiffened panels are characterized by high web heights, and their deformation is governed by the stationary hinge stage. The ALE simulations demonstrate that the magnitude of the initial peak pressure does not influence much the structural responses. It is the impulse i.e. the area under the pressure-time curve that matters.

The good correlation with both experiments and numerical simulations demonstrates the robustness and validity of the hydro-plastic model to predict the

large deflection response of plates and stiffened panels. The non-dimensional diagrams from the hydroplastic model are good candidates to be utilized in rules and standards concerned with design against extreme water slamming in ALS conditions.

## ACKNOWLEDGEMENT

The authors gratefully acknowledge the financial support by Research Council of Norway via the Centers of Excellence funding scheme, project number 223254 – NTNU AMOS. The authors would also like to thank the support from high performance computation resources from the Norwegian national e-infrastructures, Project NN9585K - Accidental actions on strait crossings and offshore platforms.

## REFERENCES

- ABRAHAMSEN, B. C., ALSOS, H. S., AUNE, V., FAGERHOLT, E., FALTINSEN, O. M. & HELLAN, Ø. 2020. Hydroplastic response of a square plate due to impact on calm water. *Physics of Fluids*, 32, 082103.
- BISHOP, R. E. & PRICE, W. G. 1979. *Hydroelasticity of ships*, Cambridge University Press.
- CHEON, J. S., JANG, B.-S., YIM, K. H., LEE, H. D., KOO, B.-Y. & JU, H. 2016. A study on slamming pressure on a flat stiffened plate considering fluid–structure interaction. *Journal of Marine Science and Technology*, 21, 309-324.
- DNVGL-OTG-13 2016. Prediction of air gap for column stabilised units. *offshore technical guidance*.
- DNVGL-OTG-14 2016. Horizontal wave impact loads for column stabilised units. *Offshore Technical Guidance*.
- FALTINSEN, O. M. 2000. Hydroelastic slamming. *Journal of Marine Science and Technology*, 5, 49-65.
- HENKE, D. J. 1994. Transient response of plates to travelling loads with application to slamming damage. *International journal of impact engineering*, 15, 769-784.
- JIANG, J. & OLSON, M. 1995. Rigid-plastic analysis of underwater blast loaded stiffened plates. *International journal of mechanical sciences*, 37, 843-859.
- JONES, N. 2011. *Structural impact (second edition)*, Cambridge university press.
- KVALSVOLD, J. & FALTINSEN, O. M. 1995. Hydroelastic modelling of wet deck slamming on multihull vessels.
- QIN, Z. & BATRA, R. C. 2009. Local slamming impact of sandwich composite hulls. *International Journal of Solids and Structures*, 46, 2011-2035.

- TRUONG, D. D., JANG, B.-S., JU, H.-B. & HAN, S. W. 2020. Prediction of slamming pressure considering fluid-structure interaction. Part I: numerical simulations. *Ships and Offshore Structures*, 1-22.
- YU, Z., AMDAHL, J., GRECO, M. & XU, H. 2019a. Hydro-plastic response of beams and stiffened panels subjected to extreme water slamming at small impact angles, Part I: An analytical solution. *Marine Structures*, 65, 53-74.
- YU, Z., AMDAHL, J., GRECO, M. & XU, H. 2019b. Hydro-plastic response of beams and stiffened panels subjected to extreme water slamming at small impact angles, part II: Numerical verification and analysis. *Marine Structures*, 65, 114-133.
- YU, Z., AMDAHL, J. & SHA, Y. 2018. Large inelastic deformation resistance of stiffened panels subjected to lateral loading. *Marine Structures*, 59, 342-367.